ISSN : 0974 - 7486 Volume 7 Issue 3

Trade Science Inc.

Materials Science

An Indian Journal

Full Paper

MSAIJ, 7(3), 2011 [184-192]

As-cast microstructures of {M - 30Cr - 0 to 5% C} ternary alloys. Part III: Iron-base alloys

Patrice Berthod[1,2,*], Ahmed Dia[1], Moussa Ba[1]

[1]Faculty of Sciences and Technologies, B.P. 70239, 54506 Vandoeuvre-lès-Nancy, (FRANCE)

[2]Institut Jean Lamour (UMR 7198), Department of Chemistry and Physics of Solids and Surfaces, B.P. 70239, 54506 Vandoeuvre-lès-Nancy, (FRANCE)

E-mail : Patrice.Berthod@lcsm.uhp-nancy.fr

Received: 14th October, 2010 ; Accepted: 24th October, 2010

ABSTRACT

As seen before with nickel alloys and cobalt alloys in the two first parts of this work, it was found again here that high carbides fractions can be also achieved in iron-based alloys if they contain sufficient quantities of carbon. With the simple ternary Fe-30Cr based alloys studied here, as predicted by thermodynamic calculations, a wide range of fractions of chromium carbides was really observed since more than 50% of carbides, in mass or volume fraction, were observed in the 5wt.%C-containing alloy, which was still free of any precipitated graphite. If carbides were only in the interdendritic eutectic form for the low carbon alloys, additional pro-eutectic carbides are present in alloys containing more than 3wt.%C. Very high values of hardness can be then also expected with such carbon-rich iron(+chromium) alloys, as for the cobalt-based alloys, by comparison with the nickel-based ones in which graphite was present for carbon contents higher than 3.5wt.%.

© 2011 Trade Science Inc. - INDIA

KEYWORDS

Iron alloys;
High chromium;
Very high carbon;
Thermodynamic calculations;
Solidification;
Microstructure.

INTRODUCTION

Carbon-containing iron-based alloys are generally known to possibly offer great volume fractions of hard phases which allow leading to high hardness values, as cementite, pearlite or martensite. Such hard phases or compounds can be easily obtained by a fast solidification[1,2] (eventually facilitated by the presence of carbide-former elements in the alloy's chemical composition), by a fast cooling from the austenite domain[3] (similarly helped by the presence of pearlite-stabilizer elements if necessary) and water quenching from the austenitic domain[4], respectively. If chromium is added to their chemical composition the hardness of bulk[5] or of hardfacing coating[6] iron-based alloys can reach high levels, for example by the formation of numerous interdendritic chromium carbides.

In this work, which is the third and final part of a study the two first parts of which dealt with nickel-30wt.% chromium – 0 to 5wt.% carbon[7] and cobalt-30wt.% chromium – 0 to 5wt.% carbon[8] systems, thirteen binary/ternary iron-based alloys, containing the same chromium and carbon amounts as the previous alloys, were considered. Similarly as what it was previously done for the Ni-30Cr-0 to 5C and Co-30Cr-0 to 5C alloys, the solidification sequences and the

possible solid transformations during cooling were studied with preliminary thermodynamic calculations. The real alloys were thereafter effectively elaborated by foundry and their microstructures characterized by metallography.

EXPERIMENTAL

Initial thermodynamic calculations

The microstructures of the alloys were firstly anticipated by thermodynamic calculations, prior to real elaborations. This exploration of the theoretic microstructures was carried out by using the N-version of the Thermo-Calc software[9] and a database containing the descriptions of the Fe-Cr-C system and its sub-systems[10-16]. The stable state microstructures were determined for all temperatures between 1500°C and 0°C, step 100°C, here too taking in mind that only the ones calculated for temperatures high enough can be really encountered for real alloys.

Elaboration and metallographic characterization of the alloys

As for the nickel alloys and for the cobalt alloys of the first and second parts of this work, the carbon contents of the thirteen Fe-30wt.%Cr-xC alloys considered here are equal to 0 (alloy named "Fe00"), 0.2 (Fe02), 0.4 (Fe 04), 0.8 (Fe 08), 1.2 (Fe 12), 1.6 (Fe 16), 2.0 (Fe 20), 2.5 (Fe 25), 3.0 (Fe 30), 3.5 (Fe 35), 4.0 (Fe 40), 4.5 (Fe 45) and 5.0 wt.%C (Fe 50). They were elaborated by foundry from pure elements (iron and chromium: Alfa Aesar, purity higher than 99.9 wt.%; carbon: graphite). These elements were melted together under an inert atmosphere of 300mbars of Argon U to prevent any loss of element because of oxidation, and a 30g-ingot of each alloy was obtained. Fusion and solidification were achieved in the water–cooled copper crucible of a CELES high frequency induction furnace. The obtained ingots were cut, embedded in a cold resin mixture and polished with SiC paper from 240 to 1200 grit and finished using a textile disk enriched in 1µm diamond particles.

A Scanning Electron Microscope (SEM: Philips, model XL30) was used for the metallographic characterization, mainly in the Back Scattered Electrons mode (BSE, 20kV). Several micrographs were taken at magnification ×500 or ×1000, to illustrate the obtained microstructures as well as to estimate the surface fractions of the different phases by image analysis (software Adobe Photoshop CS).

RESULTS AND DISCUSSION

Thermodynamic calculations

Figure 1 presents the curves describing the evolution of the mass fractions of the calculated stable states of the nearly eutectic Fe30 alloy when temperature decreases from 1500°C to 1400°C, then 1300°C etc..., as determined by Thermo-Calc calculations. This alloy was preferred instead the binary Fe00 (already fully solid at 1500°C) to show that such graph can be used, at least qualitatively, to approximately know the microstructure development of the alloy during solidification and the solid state cooling (for temperatures not too low). In the present case solidification obviously occurs near about 1300°C, with the appearance, almost simultaneously, of a FCC iron matrix containing a part of chromium and of Cr_7C_3 chromium carbides. This type of microstructure remains until temperature decreases to about 1000°C, temperature at which a very small quantity of $M_{23}C_6$ carbides may appear (before disappearing again about two hundreds degrees lower), just before the allotropic change of the austenitic FCC matrix into a ferritic BCC one. At low temperature (near 300°C), the Cr_3C_2 carbides may appear if kinetics of diffusion and/or transformation rates could be still sufficient.

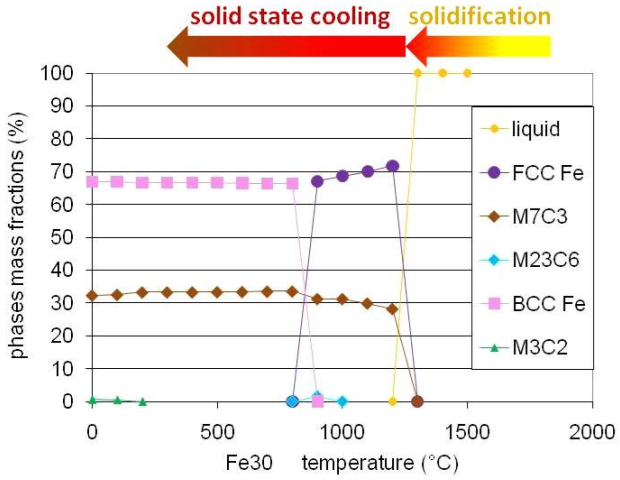

Figure 1 : Stable metallurgical states of the Fe30 alloy as calculated by Thermo-Calc; qualitative illustration of the microstructure development during solidification and cooling

Full Paper

The phase transformations during the post-solidification cooling of the binary Fe00 alloy (its solidification occurred at temperatures higher than 1500°C) and during both solidification and solid state cooling of the low carbon hypoeutectic ternary alloys (Fe02 to Fe08) can be described by the graphs of the same kind presented in figure 2. The solidification of all these alloys begins by the crystallization of the BCC matrix at a high temperature (near 1500°C), which finishes by the appearance of eutectic $M_{23}C_6$ carbides in addition. The latter are logically more present when the carbon content of the alloy is higher. They remain with these mass fractions during the cooling down to low temperatures (from 3.5% for Fe02 to 14% for Fe08, in mass) while a part of matrix, in the same time, changes two times: the first one into a FeCr phase (near 800°C for Fe02, temperature decreasing to near 600°C for Fe08) and the second one near 400°C where the sigma phase disappears while an almost pure Cr HCP phase appears.

This solidification of matrix followed by eutectic $M_{23}C_6$ occurs also for the Fe12 and Fe16 alloys, as displayed in Figure 2, while the appearance of a sigma phase at low temperature has become discrete (Fe12) or even does not occur any more (Fe16); however these two alloys are possibly still affected by the appearance of the Cr-rich HCP at very low temperature. Carbides are always $M_{23}C_6$ (in mass: 21% for Fe12 and 28% for Fe16). The high temperature transformation of the BCC matrix into FCC matrix which partly occurs for Fe16 just after the BCC solidification, is totally replaced by the solidification of matrix directly with the FCC form for the Fe25 alloy which is the C-richest alloy of this study to display a hypoeutectic character. For the Fe20 and Fe25 alloys the low temperature sigma phase and pure Cr HCP phase never precipitate while the amounts of carbides are already high (between 30 and 40% in mass). The $M_{23}C_6$ type is progressively partly replaced by the C-richer Cr_7C_3 sort during the cooling from a medium

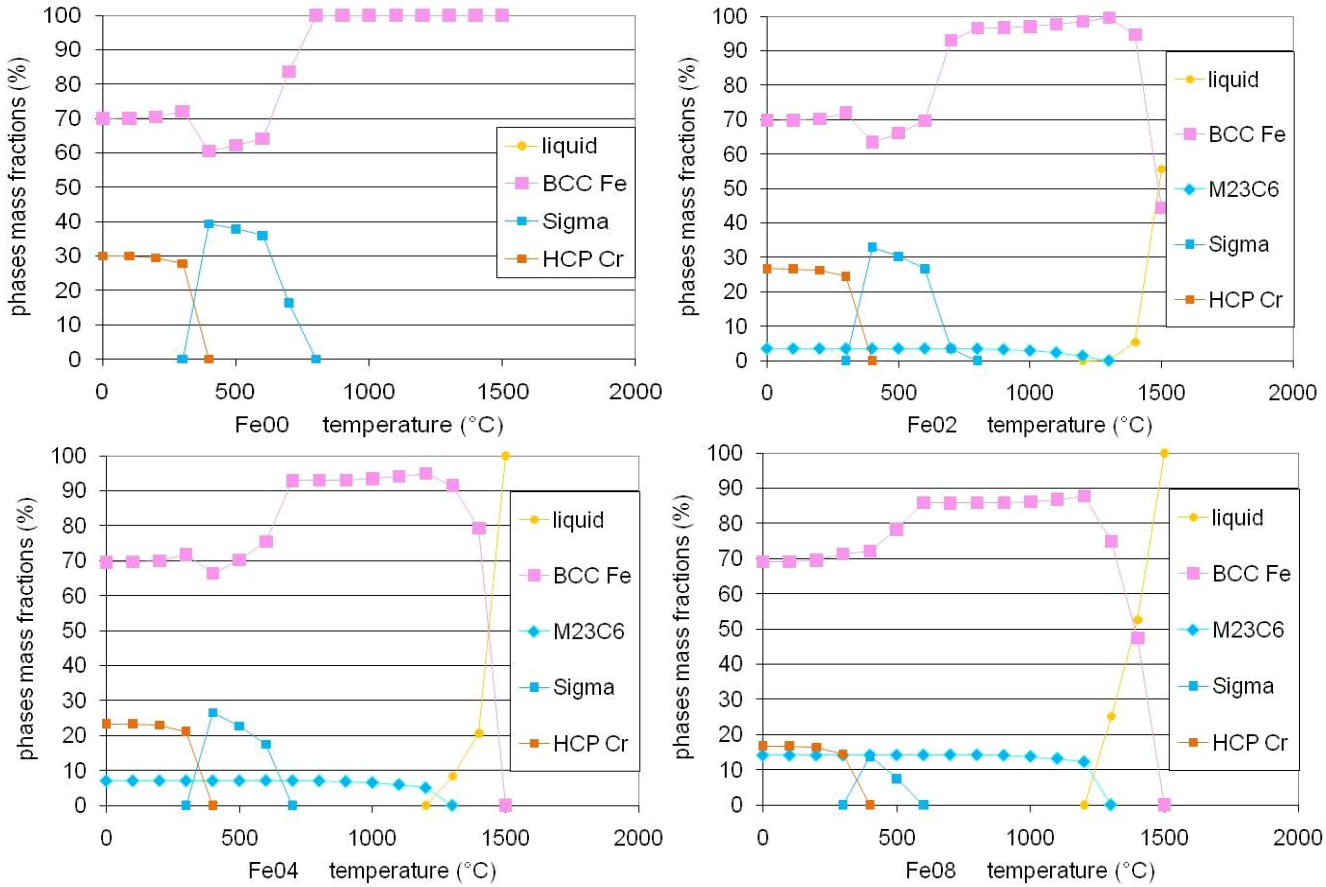

Figure 2 : Stable metallurgical states of the low carbon hypo-eutectic Fe02 to Fe08 alloys as calculated by Thermo-Calc; qualitative illustration of the microstructures development during solidification and cooling

temperature which increases when the carbon content in the alloy increases (from about 500°C for Fe20 to near 900°C for Fe25). One can notice that it is the Cr_7C_3 type which tends to appear at the end of solidification in the case of the Fe25 alloy, for which they seemingly disappear for forming $M_{23}C_6$ carbides (more than 40% in mass) before appearing again near 900°C. For the Fe25 alloy, half of the carbides population is Cr_7C_3 at medium temperatures, which induces a decrease in total carbide fraction because of the carbon content greater in Cr_7C_3 than in $M_{23}C_6$. The eutectic solidification may be obviously observed for about 3wt.%C, as displayed in the graph presented above for the Fe30 alloy (Figure 1). Solidification and solid state phase transformations of this alloy were commented above. One can just notice that the carbide type present over the whole considered temperature range is Cr_7C_3, with a mass fraction near 33.5%.

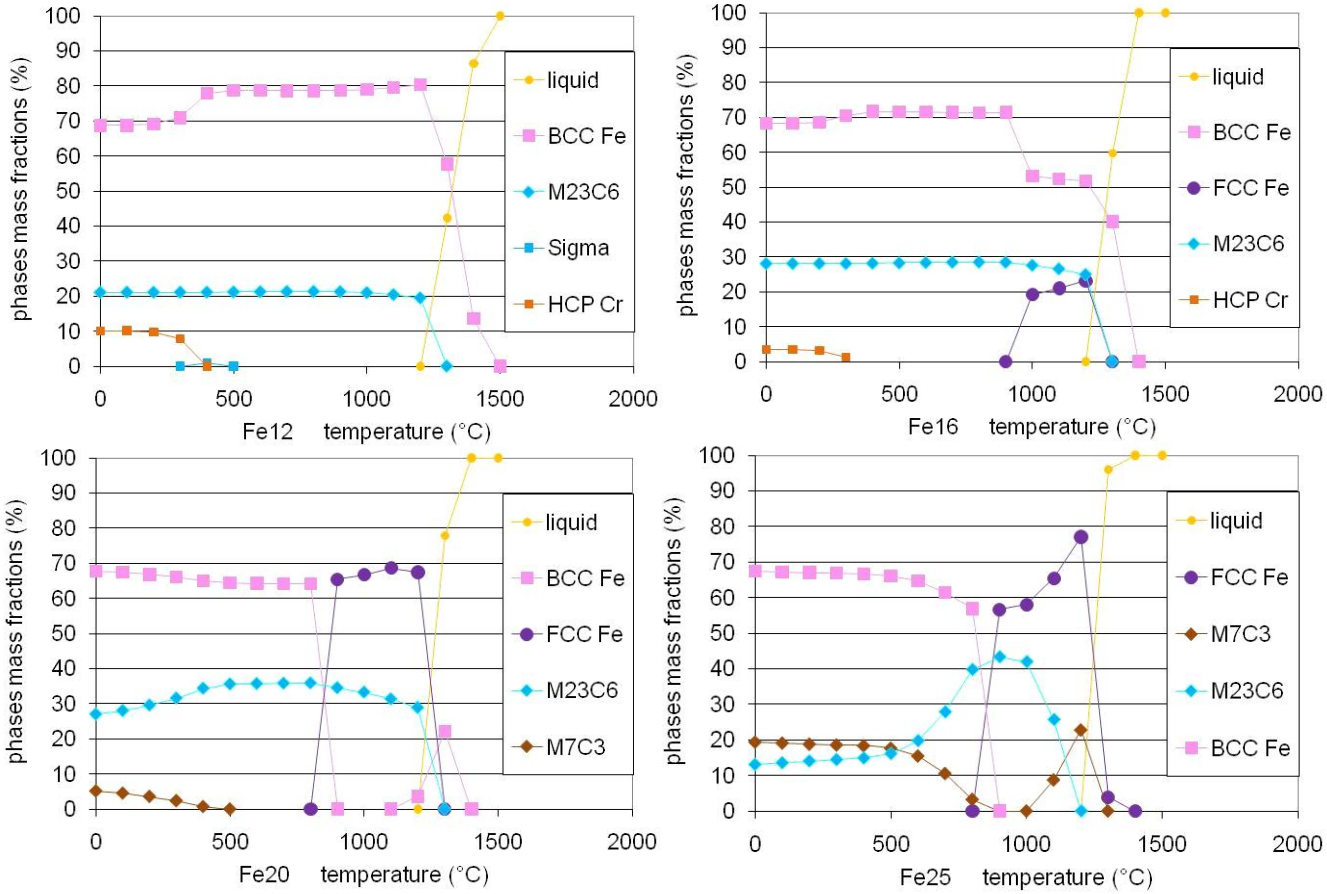

Figure 3 : Stable metallurgical states of the high carbon hypo-eutectic Fe12 to Fe25 alloys as calculated by Thermo-Calc; qualitative illustration of the microstructures development during solidification and cooling

For the highest carbon contents, solidification starts with the crystallization of carbides instead matrix. Indeed the Cr_7C_3 carbides are the first solid phase to appear, followed by the eutectic containing both Cr_7C_3 and the FCC matrix. During the solid state cooling two main transformations occur: first the replacement of the austenitic FCC form by the ferritic BCC form over a short temperature range approximately centred on about 700°C and decreasing when the carbon content increases, and the replacement of a part of the Cr_7C_3 carbides (or all of them for Fe50) by the richer Cr_3C_2 ones when temperature has decreased to about 500°C. As the lower C alloys (Fe20 and Fe25) when the $M_{23}C_6$ carbides were replaced by the Cr_7C_3 ones, this replacement of the Cr_7C_3 by the Cr_3C_2 ones induces a decrease in carbides mass fraction. However the mass fractions of carbides are very high for this high carbon contents; notably, for the Fe50 the Cr_7C_3 at high temperature are more present than the matrix itself (57% in mass at 600-700°C) but they are totally transformed into 35% in mass of Cr_3C_2 under 600°C while a very small quantity of graphite appears for the same temperature.

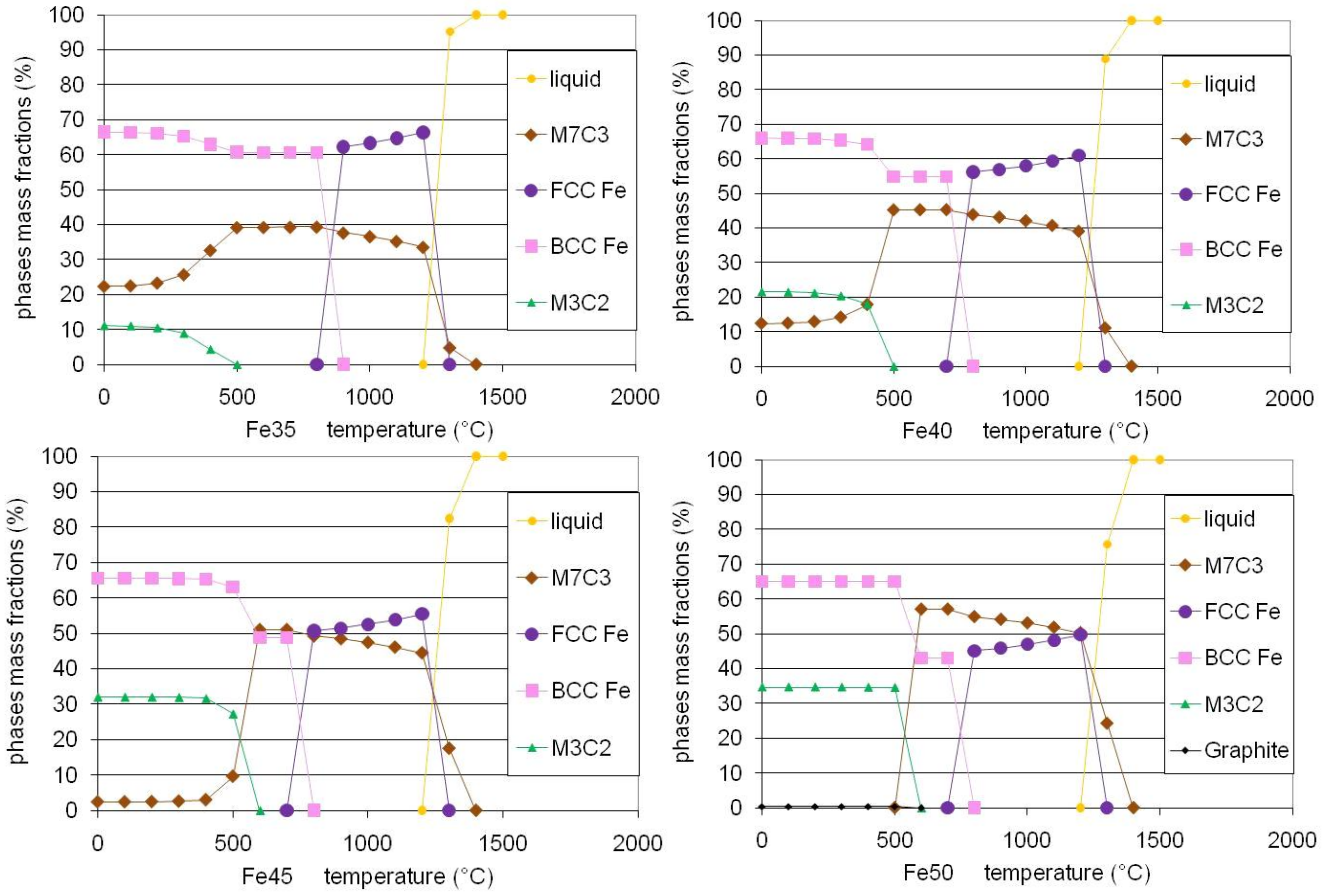

Figure 4 : Stable metallurgical states of the hyper-eutectic Fe35 to Fe50 alloys as calculated by Thermo-Calc; qualitative illustration of the microstructures development during solidification and cooling

As-cast microstructures of the elaborated alloys

Figure 5, figure 6 and figure 7 display the as-cast microstructures respectively of the Fe02 to Fe12 alloys (low carbon contents and hypo-eutectic compositions), of the Fe16 to Fe30 (high carbon contents and hypo-eutectic compositions as well as the eutectic one) and of the hyper-eutectic alloys Fe35 to Fe50. With the presence of dendrites (better seen in the alloys containing 0.4wt.C and more) the Fe02 to Fe25 alloys have microstructures effectively resulting of a hypo-eutectic solidification. The eutectic value of carbon content seems close to 3wt.% since rare dendrites and rare coarse carbides can be seen here and there in the Fe30 microstructure while the major part of this alloy is obviously constituted of a rather fine eutectic-type compound in which matrix and fine carbides are mixed together. For higher carbon contents, coarse carbides become more important and numerous, with consequently apparent greater carbides fractions. Concerning the population of carbides (appearing darker than matrix when observations are realized using the SEM in BSE mode), it is evident that their surface fraction increases when the increase in carbon.

These metallographic observations are qualitatively in great accordance with the thermodynamic calculations earlier presented, concerning the following points:

- the BCC (low carbon) or FCC (high carbon) iron dendrites are the first solid phase to appear at the beginning of solidification for the lowest carbon contents in the studied range (which changes for carbon contents higher than 3wt.%),
- the change in first phase to crystallise from 2.5wt.% (matrix) to 3.5wt.% (Cr_7C_3 carbide), with a eutectic value of carbon content near 3wt.%,
- the carbide fraction logically increases with the carbon content.

There is nevertheless a point of qualitative disagreement between calculations and real obtained alloys: the presence of graphite when the carbon content is especially high. Indeed, appearance of a very small

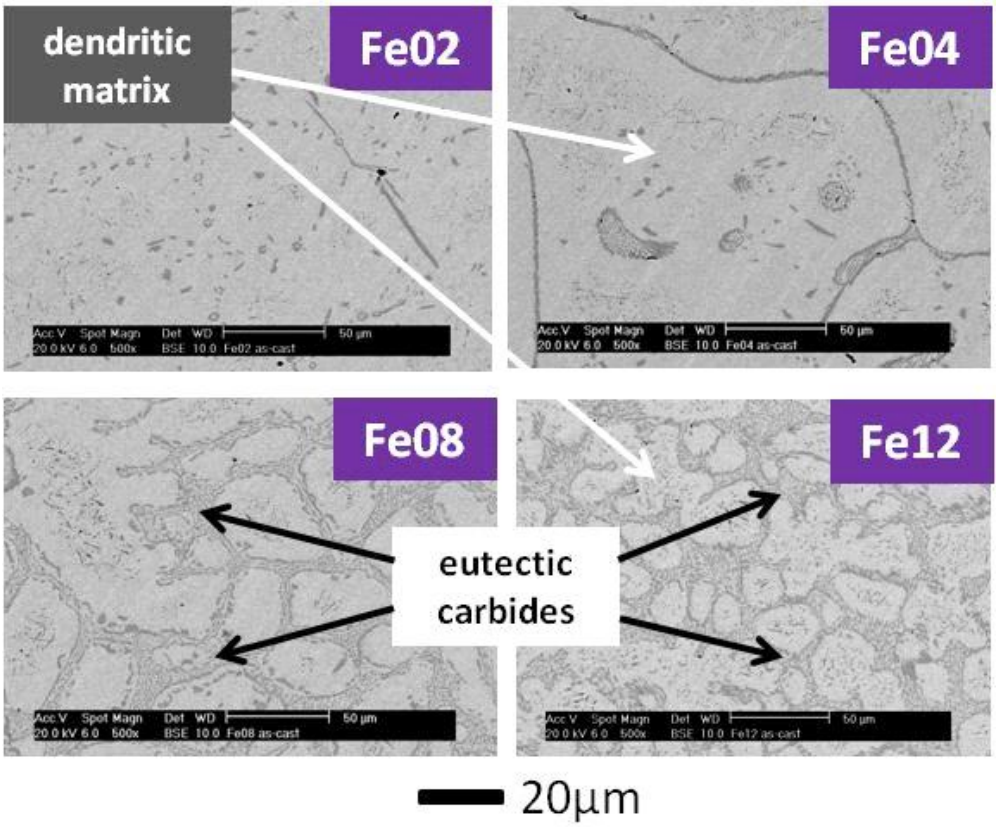

Figure 5 : As-cast microstructures of the low carbon hypo-eutectic alloys (Fe02 to Fe12)

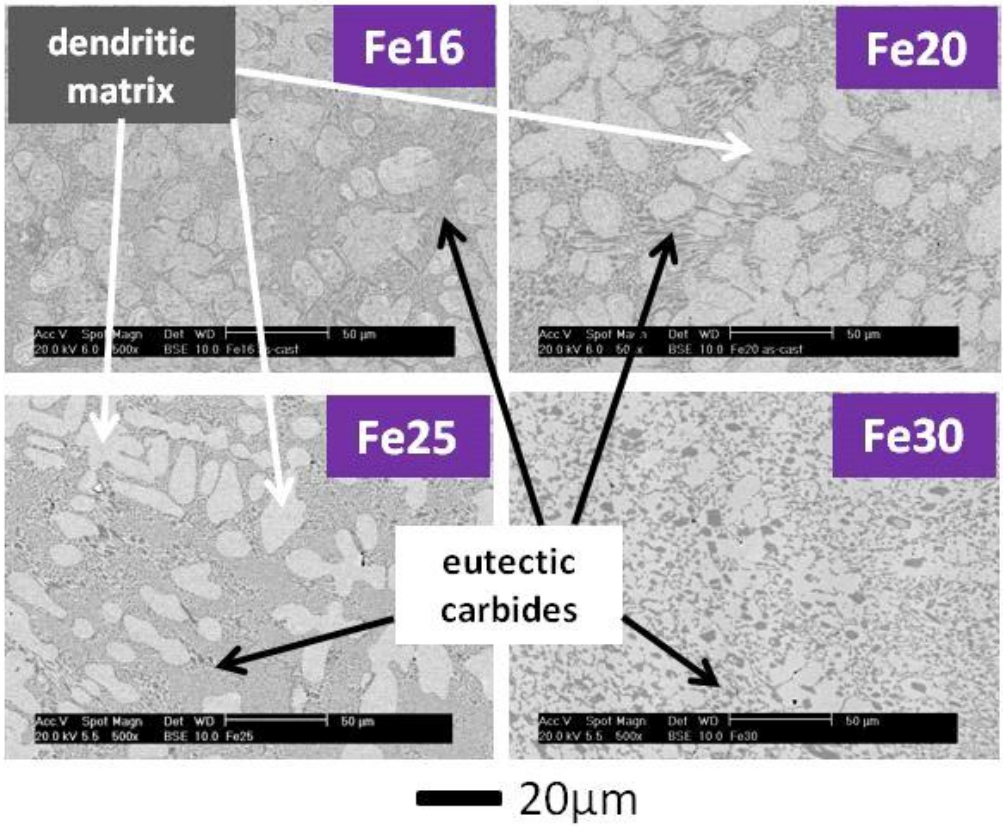

Figure 6 : As-cast microstructures of the high carbon hypo-eutectic alloys (Fe16 to Fe30)

quantity of graphite was predicted by calculations (solid state transformation in the Fe50 alloy at low temperature) while no graphite was observed in the real Fe50 alloy.

The agreement is generally good between the carbides mass fractions issued from calculations and the ones deduced from the surface fractions of carbides observed in the centres of the ingots determined by image analysis. The latter were performed, with Photoshop, generally for pictures taken at ×500 or ×1000, and the surface fractions, assumed to be close to the volume fractions, were converted in mass fractions using 6.86 g/cm^3 for carbides (average of the densities of all types of carbides[17]: 6.97 ($M_{23}C_6$), 6.92 (M_7C_3), 6.68 (M_3C_2), 8.07 (cementite Co_3C) g/cm^3, 7.29 g/cm^3 for matrix.

This can be evidenced by the following comparisons between the as-cast phase fractions of carbides and the predicted ones:

- Fe02 alloy: 4.08 surf.% of carbides, as is to say 3.85 mass.% (to compare to 1.5 – 3.6 mass.% calculated depending on temperature),
- Fe04 alloy: 6.14 surf.% of carbides, i.e. 5.80 mass.% (to compare to 5.0* – 7.1** mass.% calculated),
- Fe08 alloy: 15.7 surf.% of carbides, i.e. 14.9 mass.% (to compare to 12.3 – 14.2 mass.% calculated),
- Fe12 alloy: 19.8 surf.% of carbides, i.e. 18.8 mass.% (to compare to 19.5 – 21.4 mass.% calculated),
- Fe16 alloy: 25.0 surf.% of carbides, i.e. 23.9 mass.% (to compare to 25.0 – 28.6 mass.% calculated),
- Fe20 alloy: 23.4 surf.% of carbides, i.e. 22.3 mass.% (to compare to 28.9 – 35.9 mass.% calculated),
- Fe25 alloy: 25.2 surf.% of carbides, i.e. 24.1 mass.% (to compare to 22.9 – 43.3 mass.% calculated),
- Fe30 alloy: 28.8 surf.% of carbides, i.e. 27.5 mass.% (to compare to 28.3 – 33.6 mass.% calculated),
- Fe35 alloy: 30.4 surf.% of carbides, i.e. 29.1 mass.% (to compare to 33.6 – 39.4 mass.% calculated),
- Fe40 alloy: 37.9 surf.% of carbides, i.e. 36.4 mass.% (to compare to 39.0 – 45.2 mass.% calculated),
- Fe45 alloy: 47.9 surf.% of carbides, i.e. 46.4 mass.% (to compare to 44.5 – 51.1 mass.% calculated),
- Fe50 alloy: 54.8 surf.% of carbides (and no graphite), i.e. 53.3 mass.% (to compare to 50.3 – 57.0 mass.% and max 0.4 mass.% calculated).

(for all alloys: * just after the solidification's end, ** maximal value over the total temperature range)

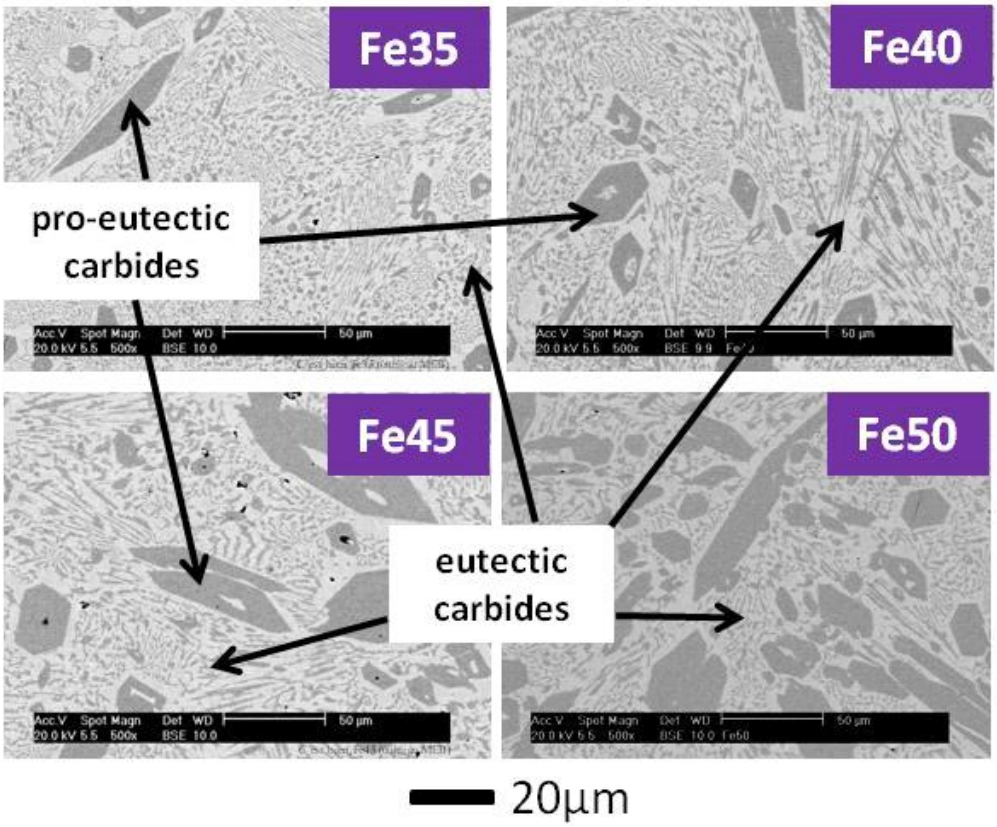

Figure 7 : As-cast microstructures of the very high carbon eutectic and hyper-eutectic alloys (Fe35 to Fe50)

General commentaries

As for the ternary nickel alloys[7] and cobalt alloys[8] containing 30wt.%Cr and the same carbon quantities as here, a wide range of carbides fractions was shown by these iron alloys. These ones can be here to eutectic carbides (hypo-eutectic alloys) and/or coarse pro-eutectic carbides (hypereutectic alloys) and their fractions can exceed 50%; the major part of the concerned alloy (Fe50) is then carbides and not more the metallic matrix. The limit in carbon content separating the hypo-eutectic and the hyper-eutectic alloys seems close to the one already determined for the cobalt alloys (near 3wt.%), and then higher than for the nickel alloys (between 1.6 and 2.0wt.%C). As for the cobalt alloys previously studied this helped to avoid too high quantities of coarse primary carbides, and then to prevent the serious problems of severe heterogeneity encountered in the case of the nickel alloys. The microstructure homogeneity was here much better than for the nickel alloys, and even better than for the cobalt alloys since no real outer part of special structure was really seen for the iron C-richest alloys.

It can be interesting to compare the mass carbides fractions obtained in the real alloys for the three systems: iron base, cobalt base and nickel base alloys, by considering the curves plotting these mass fractions versus the targeted carbon content which are displayed in figure 8. One can see that, for the lowest carbon contents, that the carbides fraction increases faster for the iron alloy than for the cobalt and nickel alloys. Since this corresponds to the solidification of the BCC iron matrix (Fe02 to Fe16) while, for higher carbon contents, the Fe-base matrix solidifies in the FCC form (as for the Co-base and Ni-base matrixes), these higher carbides fractions for the iron alloys appear to be possibly attributed to this solidification of matrix with the BCC form. Indeed, for carbon contents for which the matrix solidifies in the FCC form, the carbides fractions are quite similar for the three types of alloy (Fe-, Co- and Ni-based) for a same carbon content (2.0 to 3.5wt.%), except for the Co20 alloy for which the carbides fraction is curiously very low for such a carbon content. For higher carbon contents, the curves become different again: carbides fractions of the nickel alloys significantly lower than for the cobalt alloys and the iron alloys (3.5 to 5.0wt.%C), and for the Co50 alloy by comparison for the Fe50 one. This is due to the precipitation of graphite in the Ni35 to Ni50 alloys and maybe also for the Co50 alloy despite graphite was not clearly evidenced. Such graphite appearance evidently leads to much more carbon available to form carbides.

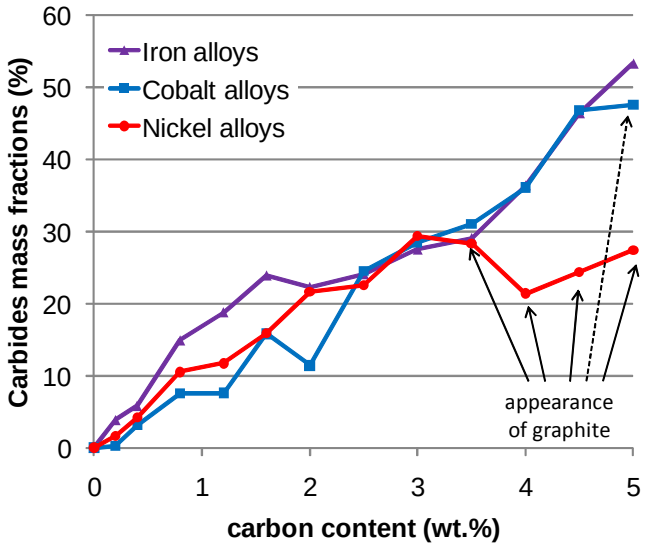

Figure 8 : Comparison between the carbides mass fractions really obtained in the studied alloys for the three base elements: iron, cobalt[8] and nickel[7]

CONCLUSIONS

In this third family of {30wt.%Cr + carbon} containing alloys too, very high carbides fractions can be obtained by adding sufficiently carbon. It is in this iron-based alloys family that the maximal volume or mass fractions were met, as high as more than 50% in the Fe-30Cr-5.0C alloy, without detectable precipitation of graphite. This let think that very high levels of hardness can be expected. Thus, the three systems studied along the three articles of this series can offer numerous candidates of more or less expensive alloys (depending on the base element), all of them easily to elaborate by foundry, for applications needing very high values of hardness.

ACKNOWLEDGEMENTS

The authors thank Lionel Aranda and Thierry Schweitzer for their technical assistance.

REFERENCES

[1] G.Lesoult; 'Solidification: Cristallisation et microstructures', Techniques de l'ingénieur, M58, Paris **(1986)**.

[2] W.Kurz, D.J.Fisher; 'Fundamentals of Solidification', Trans.Tech.Publ., Switzerland **(1989)**.

[3] M.Durand-Charre; 'Microstructure of Steels & Cast Irons (Engineering Materials & Processes)', Springer **(2004)**.

[4] A.Litwinchick, F.X.Kayser, H.H.Baker, A.Henkin; J.Mater.Sci., **11**, 1200 **(1976)**.

[5] H.E.N.Stone; J.Mater.Sci., **14**, 2781 **(1979)**.

[6] B.V.Cockeram; Met.Mater.Trans.A: Phys.Met. Mater.Sci., **33**, 3403 **(2002)**.

[7] P.Berthod, E.Souaillat, O.Hestin; Materials Science: An Indian Journal, (In press).

[8] P.Berthod, O.Hestin, E.Souaillat; Materials Science: An Indian Journal, (In press).

[9] Thermo-Calc version N; 'Foundation for Computational Thermodynamics' Stockholm, Sweden, Copyright (1993), **(2000)**.

[10] A.Fernandez Guillermet, P.Gustafson; High Temp.High Press, **16**, 591 **(1984)**.

[11] J.-O.Andersson; Int.J.Thermophys., **6**, 411 **(1985)**.

[12] P.Gustafson; Carbon, **24**, 169 **(1986)**.

[13] J.-O.Andersson, B.Sundman; Calphad, **11**, 83 **(1987)**.

[14] P.Gustafson; Scan.J.Metall., **14**, 259 **(1985)**.

[15] J.-O.Andersson; Calphad, **11**, 271 **(1987)**.

[16] J.-O.Andersson; Met.Trans.A, **19A**, 627 **(1988)**.

[17] G.V.Samsonov; 'Handbooks of High-Temperature Materials N°2. Properties Index', Plenum Press, New York **(1964)**.